PVDF/NICKEL COMPOSITES AND THEIR CHARACTERIZATION

S.M. Lebedev*, O.S. Gefle
Tomsk Polytechnic University, Russia
2A Lenin Avenue, 634028, Tomsk, RUSSIA
*e-mail: lsm70@mail.ru

Abstract: PVDF/metal submicro- and nanocomposites were prepared by means of a mixing in twin screw extruder and planetary ball mill, respectively. All samples were prepared by hot pressing method. Their electrical, thermal and structural properties were examined by dielectric spectroscopy, DSC, FTIR, XRD, optical microscopy and scanning electron microscopy. Properties of composites were found to be strongly modified depending on the content of metal powders and filler particles size. Particularly, specific volume resistivity of PVDF/Ni composite at 0.2 wt% of Ni was increased by a factor of 1.5…4 compared to that for pure PVDF.

1 INTRODUCTION

Filling a polymeric matrix by filler powder results in the modification of both the polymer structure and properties of composite materials due to formation of interface at the boundary matrix/filler particles [1, 2]. Adding of submicro- and nanosized fillers into polymeric matrixes may result in enhancement or stabilization of electrical, mechanical and thermal properties of polymeric dielectrics due to the increase in the interphase interaction at the boundary matrix/filler [3–7].

Polyvinylidene fluoride (PVDF) is widely used as a matrix for the composite polymeric materials (CPM's) with required properties [4–7]. This polymer possesses a high operating temperature and dielectric strength. High permittivity of PVDF allows achieving both uniform distribution of a local electric field in filled materials and a low dispersion of the complex permittivity at the required frequency range.

Nickel is chemically the more stable metal and therefore its application in polymer/metal composites as a modifying agent is preferable compared to other metal powders such as iron, aluminum, copper, etc. Moreover usage of other metal powders mentioned above can result in acceleration of thermo-oxidative destruction of polymeric matrices especially halogenated polymers [8].

It is well known that usage of submicro- and nanosized metal powders as fillers can change mechanical, magnetic and electrical properties of polymeric composites in spite of the high conductivity of metal filler [8–11]. According to [9] the adding of 3.5 wt% nickel powder into polypropylene results in the reduction of spherulite sizes by a factor of 2 compared to that for a pure polypropylene due to the formation of artificial nucleation centers [8]. The author [8] has observed an increase of the tensile strength at break of a composite material. The elastic and magnetic properties of natural rubber/nickel composites showed an improvement with increase in nickel content [11]. The permittivity of these composites was found to be increased with increase in nickel loading.

The study of electrical, thermal and structural properties of PVDF/Ni composites is the objective of this work.

2 EXPERIMENTAL PROCEDURE AND SAMPLES

Measurements of the real part ε' of the complex permittivity and loss factor tanδ were carried out under AC voltage 3V in the frequency range from 10^{-2} Hz to 1 MHz by using the Solartron Instrument (Impedance/Gain-Phase Analyzer Solartron 1260+Dielectric Interface Solartron 1296) [12]. From five to ten measurements per decade over the frequency range were carried out for all samples.

The volume resistivity ρ_v was determined under DC voltage according to IEC 60093 and ASTM D257 test standards. Each sample was placed between two electrodes. For sixty seconds, a DC voltage was applied and the resistance was measured at all requested temperatures. The volume resistivity was calculated for each measurement. Not less than five samples for each composite material were tested.

Temperatures and temperature intervals of melting and decomposition of CPM's, the heat flow and a weight loss of samples were measured in the temperature range from 25 to 500°C at a heating rate of 3–10°C/min in an argon atmosphere by means of a combined DSC-DTA-TGA analyzer Q600 "TA Instruments". From three to five samples of each composite were tested for all test conditions.

FTIR analysis was carried out by means of IR spectrometer Nicolet 5700 at the wavenumber range from 4000 to 400 cm^{-1}.

X-ray diffraction of PVDF and nanocomposites was studied by means of diffractometer Shimadzu XRD-6000.

Morphology of PVDF/metal composites was studied under cross polarized light by means of an optical microscope and a scanning electron microscope. Five samples of each composite material were tested.

Pellets and powder of PVDF ("Fluoropolymer" Ltd., St-Petersburg, Russia) was used as-received as a polymeric matrix in this study. Powders of Ni with average size of spherical particles of 200 and 72 nm produced by the electric explosion of Ni wires under the high electric field at Adv. Powder Techn. LLC (Tomsk, Russia) were used as fillers.

PVDF/Ni submicron composites were prepared by means of a mixing of PVDF pellets and 200 nm Ni particles in a twin-screw extruder. To prepare PVDF/Ni nanocomposites, PVDF powder was filled with 72 nm Ni particles by means of a mixing in a planetary ball mill. Content of Ni powder in composites was changed from 0.05 to 10.0 wt%. All samples were prepared by hot pressing in a hydraulic press. Samples studied were prepared as discs 75 mm in diameter and thicknesses of 20-150 μm.

3 EXPERIMENTAL RESULTS AND DISCUSSION

3.1 PVDF/Ni submicron composites

Temperature-frequency dependencies of ε' and $\tan\delta$ for PVDF and PVDF/Ni composites with average Ni-particles size of 200 nm are shown in Figure 1.

The values of $\tan\delta_{max}$ for composite PVDF/0.2%Ni and PVDF do not practically differ at T = 80°C and 100°C. The further increase in Ni content to 2 wt% results in the increase of $\tan\delta_{max}$ while the $\tan\delta$ peak position is practically unchangeable. Modification of PVDF matrix by 0.2…2.0 wt% of Ni does not result in visible increase of the real part ε' of the complex permittivity.

Table 1 represents the temperature dependencies of the volume resistivity ρ_v for PVDF/Ni composites with average Ni-particles size of 200 nm. It can be seen that ρ_v for composite with 0.2 wt% of Ni in the temperature range from 25°C to 80°C is increased by a factor of 1.24…15 compared to that for pure PVDF. Similar effect is observed for composite with 0.5 wt% of Ni the only difference being that the increase in ρ_v is about 1.1…2.14 compared to that for the PVDF matrix. For other composites the increase of ρ_v becomes negligible at T > 50°C in comparison with PVDF. That is, the modification of PVDF matrix by 0.2…0.5 wt% Ni results in the increase of the volume resistivity of CPM's in the temperature range from 25°C to 80°C [13].

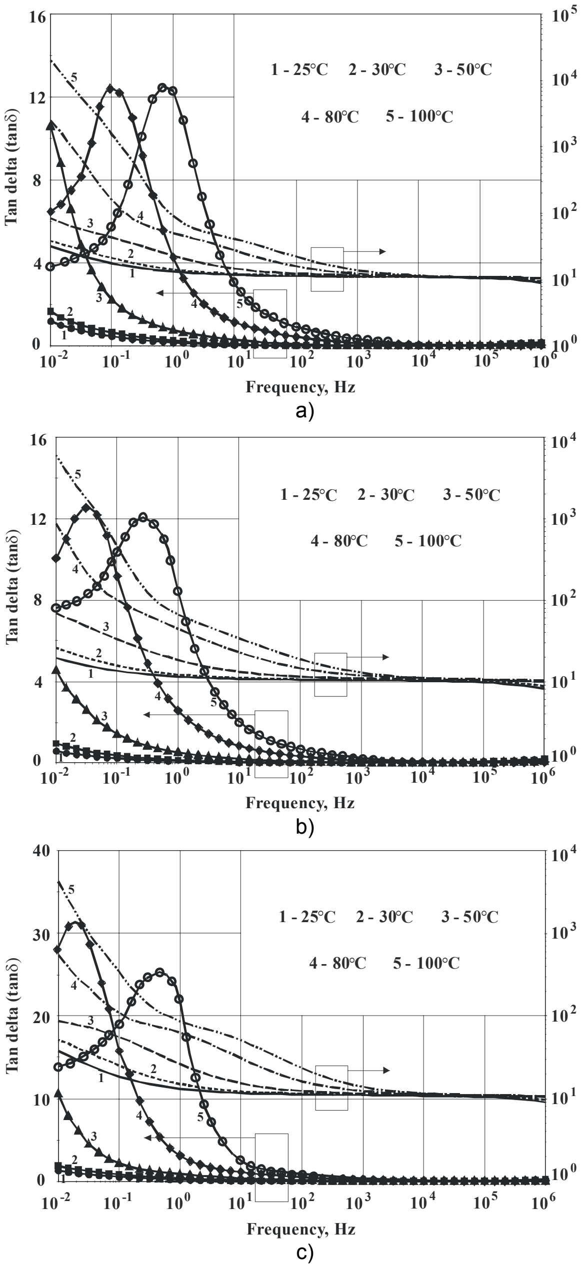

a)

b)

c)

Figure 1: Temperature-frequency dependencies of $\tan\delta$ and ε' for: a, PVDF; b, PVDF/0.2% Ni; and c, PVDF/2.0% Ni

Results of DSC/TGA analysis for pure PVDF and PVDF/Ni composites are shown in Figure 2 and Table 2 (heating rate of 3°C/min), where T_m, T_{mb}, and ΔT_m are the melting temperature, beginning melting temperature and melting interval, respectively; subscript d in Table 2 means three similar parameters for decomposition process. It can be seen that there are two endothermic processes which correspond to phase transitions in a polymeric materials. The first of them (at ~135…160°C) is related with the melting temperature of PVDF and the latter (at

~355…425°C) corresponds to the decomposition temperature.

Table 2: Thermal characteristics for PVDF/Ni submicron composites

Composite	T_{mb}, °C	T_m, °C	ΔT_m, °C
PVDF	135	152	17
PVDF/0.2% Ni	150	157	7
PVDF/0.5% Ni	144	159	15
PVDF/1.0% Ni	144	158	14
PVDF/2.0% Ni	145	159	14
	T_{db}, °C	T_d, °C	ΔT_d, °C
PVDF	356	375	19
PVDF/0.2% Ni	406	423	17
PVDF/0.5% Ni	393	424	31
PVDF/1.0% Ni	388	425	37
PVDF/2.0% Ni	383	423	40

Table 2 demonstrates that the melting temperature of PVDF/Ni composites with average Ni-particles size of 200 nm is increased by 5–7°C compared with pure PVDF. That can probably mean that the degree of crystallinity and homogeneity of sub-molecular structure for filled composites is changed compared with pure PVDF due to the formation of artificial nucleation centers [8]. The increase in Ni content in a polymer matrix from 0.2 to 2.0 wt% does not lead to considerable increase in the melting temperature for composites with Ni content more than 0.5 wt% compared to composite with 0.2 wt% of Ni. It can be caused by the formation of filler agglomerates. That is, modification of PVDF by Ni particles results in the increase of thermal stability of CPM's. Table 2 shows that the decomposition temperature T_d for filled composites is increased compared to pure PVDF and it does not practically changed with increase in Ni content. Maximum value of T_{db} is observed also for composite with 0.2 wt% of Ni. However the value of T_{db} is decreased with increase in Ni content. Such behavior of T_d and T_{db} means that agglomerates of Ni particles in CPM's are the main reason of thermal properties deterioration.

Thus, the maximum thermal stability and the higher volume of ρ_v are observed for composite with 0.2 wt% of Ni, and to some extent for 0.5 wt%, compared to PVDF. This conclusion is well confirmed also by the experimental results of the sub-molecular structure study. Figure 3 shows typical micrographs of sub-molecular structure for PVDF/Ni composites.

It can be seen that adding Ni into the polymeric matrix results in considerable modification of the PVDF sub-molecular structure. Large-size spherulite structure of PVDF matrix is transformed into a small-size spherulite one. The increase in filler content results in increase of the average size of Ni agglomerates. So, agglomerates for composites with 0.2 wt% of Ni either are absent in general or their average size does not exceed 3 μm. At 0.5 wt% of Ni the average size of Ni agglomerates is about 5 μm while at 2.0 wt% of Ni it is equals to 10…15 μm. As a result, the more homogeneous sub-molecular structure is formed in composite with 0.2 wt% of Ni [13]. That is, Ni particles may be considered as artificial nucleation centers modifying PVDF matrix [8].

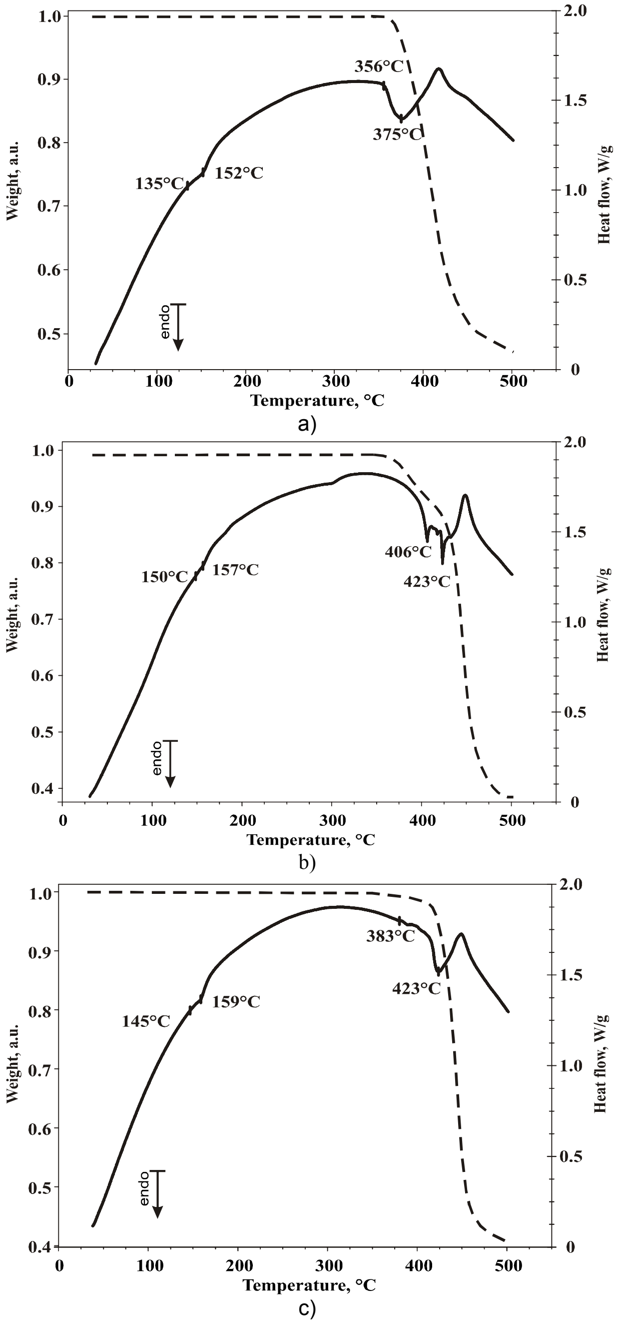

a)

b)

c)

Figure 2: DSC/TGA results for: a, PVDF matrix; b, 0.2 wt% Ni; and c, 2.0 wt% Ni; dotted line – sample weight, and solid line – heat flow

3.2 PVDF/Ni nanocomposites

To compare main properties of submicro- and nanocomposites, PVDF/Ni nanocomposites with average Ni-particles size of 72 nm were prepared. Dielectric relaxation spectra for PVDF/Ni composites with average Ni-particles size of 72 nm are shown in Figure 4. It can be seen that dielectric relaxation spectra for nanocomposites do not change compared to that for previous composites the only difference being that measurement of dielectric relaxation spectra for these composites is impossible at the Ni content more than 1 wt% because of sharp increase in the conductivity of materials. This is caused by that particles of nanofiller possess an enormous specific surface area compared to that for submicron particles and the percolation effect is observed in samples even at low Ni content (≥ 2 wt%) in nanocomposites.

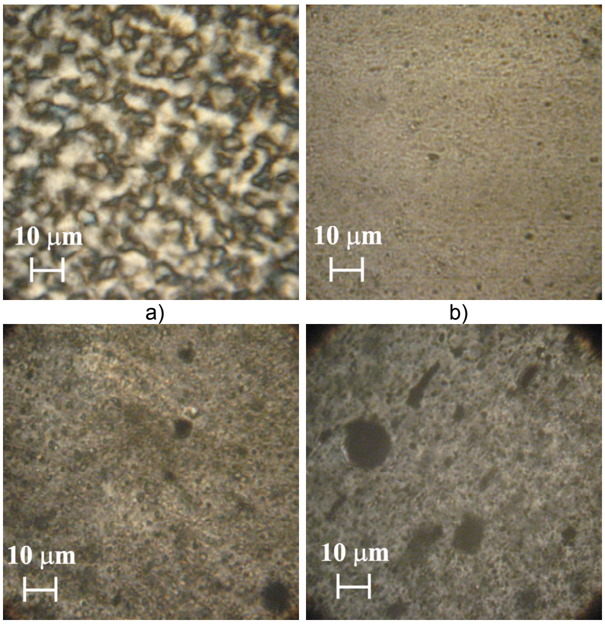

a) b)

c) d)

Figure 3: Patterns of sub-molecular structures of PVDF/Ni composites at different Ni contents: a, 0 wt%; b, 0.2 wt%; c, 0.5 wt%; and d, 2.0 wt%

Table 3 lists the activation energy *W* of the polarization process for PVDF/Ni nanocomposites. The activation energy was estimated from the temperature-frequency dependencies by means of the Arrhenius plot. It can be seen that the value of *W* is close to 1.0 eV for all nanocomposites.

Table 3: Activation energy for nanocomposites

Filler content, %	Activation energy $W \pm \sigma_W$, eV
0	0.983 ± 0.016
0.05	0.959 ± 0.011
0.1	0.986 ± 0.005
0.5	0.993 ± 0.006
1.0	1.023 ± 0.008

DSC/TGA analysis results for pure PVDF and PVDF/Ni nanocomposites are listed in Table 4 (heating rate of 10°C/min). It is obvious that the melting temperature for nanocomposites does not change with increase in the filler content from 0.05 to 5.0 wt% in contrast to submicron composites. On the other hand, the decomposition temperature T_d has been increased by 12–21°C with increase in Ni content from 0.1 to 1.0 wt%. At the high Ni content T_d has tendency to the decrease compared to that of pure PVDF. It confirm above mentioned assumption for submicron composites that deterioration of thermal properties with increase in the filler content is caused by the formation of agglomerates of Ni particles.

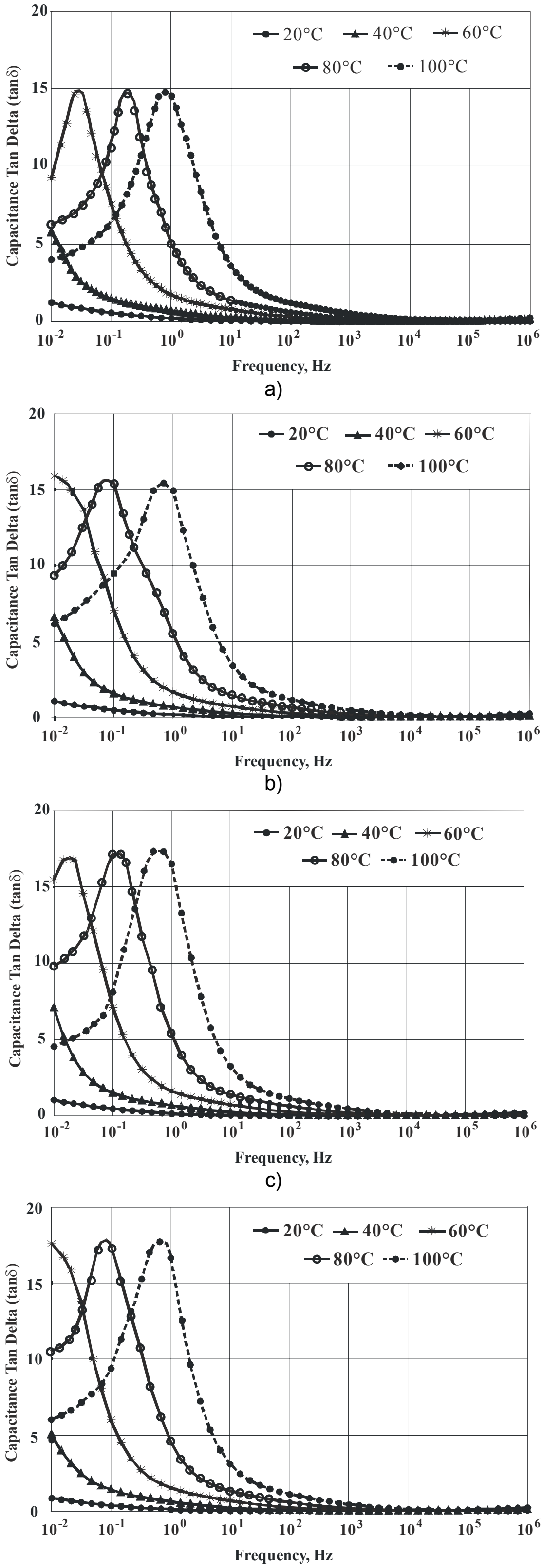

a)

b)

c)

d)

Figure 4: Dielectric relaxation spectra for pure PVDF (a) and composites with Ni content: 0.05 wt% (b), 0.2 wt% (c), and 1.0 wt% (d)

Table 4: Thermal characteristics for PVDF/Ni nanocomposites

Composite	T_{mb}, °C	T_m, °C	ΔT_m, °C
PVDF	123	159	36
PVDF/0.05% Ni	128	159	31
PVDF/0.1% Ni	128	159	31
PVDF/0.2% Ni	128	159	31
PVDF/1.0% Ni	131	160	29
PVDF/2.0% Ni	128	159	31
PVDF/5.0% Ni	127	159	32
	T_{db}, °C	T_d, °C	ΔT_d, °C
PVDF	–	430	–
PVDF/0.05% Ni	–	431	–
PVDF/0.1% Ni	–	442	–
PVDF/0.2% Ni	–	443	–
PVDF/1.0% Ni	–	451	–
PVDF/2.0% Ni	–	448	–
PVDF/5.0% Ni	–	446	–

One more interesting experimental fact has been found out when studying FTIR-spectra of pure PVDF and nanocomposites (Figure 5). For all samples prepared by hot pressing method the band centered at 1723 cm^{-1} is observed. This characteristic band can be caused by oscillations of C=C or C=O bonds of polymeric matrix. The intensity of these oscillations is decreased with increase in Ni content in nanocomposites.

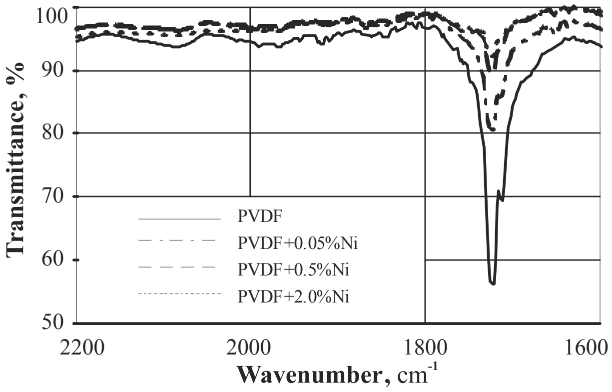

Figure 5: FTIR-spectra for pure PVDF and nanocomposites with different Ni content

The results of XRD study were used for the analysis of structural properties of PVDF/Ni nanocomposites. The X-ray diffraction patterns of pure PVDF and nanocomposites are shown in Figure 6. The weak peak centered at 18.3°, the sharp peak at 20.2° and two weak peaks at 36.1°, and 40.5° are characteristic peaks of planes (100), (020), (110) and (021) of PVDF crystallites [14]. The characteristic peaks of nickel are clearly visible at 44.4° and 51.8° [11], and the intensity of these peaks is increased with Ni content.

4 CONCLUSIONS

The main results of this study are as follows.

i) It was found that modification of PVDF by 200 nm Ni particles results in the change of sub-molecular structure of submicron composites. At low Ni content in PVDF the large-size spherulite structure of a polymeric matrix transforms into the small-size spherulite one. Ni particles are acting as an artificial nucleation agent modifying a polymeric structure.

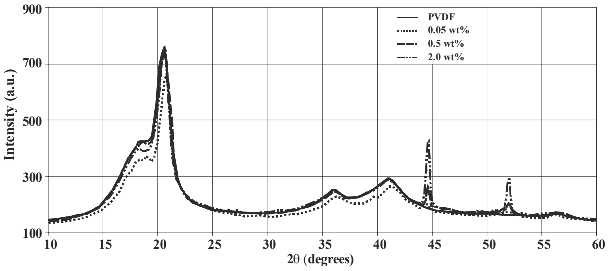

Figure 6: X-ray diffraction pattern for PVDF (a) and composites with various Ni content: 0.05 wt% (b), 0.5 wt% (c), and 2.0 wt% (d)

ii) Submicron composites with a low Ni content (less than 0.5 wt%) possess both the higher thermal stability and volume resistivity due to homogeneity of a sub-molecular structure.

iii) Decrease in the average Ni-particles size from 200 to 72 nm results in the sharp increase in the conductivity of PVDF/Ni composites due to increase of the specific surface area of filler and decrease of the percolation threshold.

iv) The number of defective bonds C=C or C=O in PVDF/Ni nanocomposites decreases with increase in Ni content. This is confirmed by the decrease in oscillations intensity of the characteristic band at 1723 cm^{-1}.

5 ACKNOWLEDGMENTS

This work was supported by the Russian Special Federal Program “Scientific and scientific-pedagogic staff of innovative Russia, 2009-2013” under the contract No. P407.

6 REFERENCES

[1] T.J. Lewis, “Nanometric dielectrics”, IEEE Trans. Diel. Elect. Ins., Vol. 1, pp. 812–825, 1994

[2] T. Tanaka, “Dielectric nanocomposites with insulating properties”, IEEE Trans. Diel. Elect. Ins., vol. 12, pp. 914–928, 2005.

[3] S.M. Lebedev, O.S. Gefle and Y.P. Pokholkov, “The barrier effect in dielectrics. The role of interfaces in the breakdown of inhomogeneous dielectrics”, IEEE Trans. Diel. Elect. Ins., Vol. 12, pp. 537–555, 2005.

[4] D.K. Das-Gupta and K. Doughty, “Polymer-ceramic composite materials with high permittivities”, Thin Solid Films, Vol. 158, pp. 93–105, 1988.

[5] H.L.W. Chan, Y. Chen and C.L. Choy, “Thermal hysteresis in the permittivity and polarization of lead zirconate titanate/ vynilidene floride-trifluoroethylene 0-3 composites”, IEEE Trans. Diel. Elect. Ins., Vol. 3, pp. 800–805, 1996.

[6] H.L.W. Chan, W.K. Chan, Y. Zhang, et al, “Pyroelectric and piezoelectric properties of lead titanate/polyvinilidene fluoride-trifluoroethylene 0-3 composites”, IEEE Trans. Diel. Elect. Ins., Vol. 5, pp. 505–512, 1998.

[7] H.L.W. Chan, Q.Q. Zhang, W.Y. Ng, et al, “Dielectric permittivity of PCLT/PVDF-TRFE nanocomposites”, IEEE Trans. Diel. Elect. Ins., Vol. 7, pp. 204–206, 2000.

[8] V.P. Solomko, Filled crystalline polymers, Naukova Dumka, Kiev, 1980.

[9] V.E. Gool, N.N. Turkova, M.G. Golubeva, “About increase in mechanical strength of conductive polymeric films filled with metals under static magnetic field”, Reports of USSR Science Academy, Vol. 199, pp. 135–137, 1971.

[10] D. Bloor, K. Donnelly, P.J. Hands, et al, “A metal-polymer composites with unusual properties”, J. Phys. D: Appl. Phys., Vol. 38, pp. 2851–2860, 2005.

[11] E.M.A. Jamal, P.A. Joy, P. Kurian, et al, “Synthesis of nickel-rubber nanocomposites and evaluation of their dielectric properties”, Mater. Sci. and Eng.: B, Vol. 156, pp. 24–31, 2009.

[12] Impedance/Gain-Phase Analyzer 1260 and Dielectric Interface 1296, User guide, 2001.

[13] S.M. Lebedev, O.S. Gefle, S.N. Tkachenko, “Metal-polymer PVDF/nickel composites and evaluation of their dielectric and thermal properties”, J. Electrostatics., Vol. 68, pp. 122–127, 2010.

[14] P. Raghavana, X. Zhaoa, J. Manuela, et al, “Electrochemical performance of electrospun poly(vinylidene fluoride-co-hexafluoropropylene)-based nano-composite polymer electrolytes incorporating ceramic fillers and room temperature ionic liquid”, Electrochemica Acta, Vol. 55, pp. 1347–1354, 2010.

Table 1: Temperature dependence of ρ_v for PVDF/Ni submicron composites

Ni content, wt%	ρ_v, Ohm·m at T, °C								
	25	30	40	50	60	70	80	90	100
0	$2.1\cdot10^{12}$	$2.2\cdot10^{11}$	$3.1\cdot10^{10}$	$4.4\cdot10^{9}$	$1.0\cdot10^{9}$	$4.6\cdot10^{8}$	$2.1\cdot10^{8}$	$1.5\cdot10^{8}$	$5.4\cdot10^{7}$
0.2	$8.2\cdot10^{12}$	$3.3\cdot10^{12}$	$4.2\cdot10^{11}$	$2.6\cdot10^{10}$	$3.3\cdot10^{9}$	$6.2\cdot10^{8}$	$2.6\cdot10^{8}$	$1.2\cdot10^{8}$	$5.8\cdot10^{7}$
0.5	$4.5\cdot10^{12}$	$4.5\cdot10^{11}$	$5.1\cdot10^{10}$	$6.8\cdot10^{9}$	$1.0\cdot10^{9}$	$5.4\cdot10^{8}$	$2.3\cdot10^{8}$	$9.8\cdot10^{7}$	$4.9\cdot10^{7}$
1.0	$2.9\cdot10^{12}$	$2.7\cdot10^{11}$	$3.1\cdot10^{10}$	$4.0\cdot10^{9}$	$6.5\cdot10^{8}$	$2.9\cdot10^{8}$	$1.3\cdot10^{8}$	$6.6\cdot10^{7}$	$3.3\cdot10^{7}$
2.0	$2.6\cdot10^{12}$	$2.9\cdot10^{11}$	$3.6\cdot10^{10}$	$5.2\cdot10^{9}$	$8.0\cdot10^{8}$	$3.3\cdot10^{8}$	$1.3\cdot10^{8}$	$6.5\cdot10^{7}$	$2.9\cdot10^{7}$